PL-TR-97-2016

THERMOSPHERIC DENSITY VARIABILITY AND FORECAST MODEL DEVELOPMENT

Jeffrey M. Forbes
Timothy Fuller-Rowell

University of Colorado
Department of Aerospace Engineering Sciences
Boulder, CO 80309

15 January 1997

Scientific Report No. 1

PHILLIPS LABORATORY
Directorate of Geophysics
AIR FORCE MATERIEL COMMAND
HANSCOM AFB, MA 01731-3010

"This technical report has been reviewed and is approved for publication"

FRANK A. MARCOS
Contract Manager

EDWARD J. WEBER
Branch Chief

DAVID A. HARDY
Division Director

This document has been reviewed by the ESC Public Affairs Office (PA) and is releasable to the National Technical Information Service (NTIS).

Qualified requestors may obtain additional copies from the Defense Technical Information Center (DTIC). All others should apply to the National Technical Information Service (NTIS).

If your address has changed, or if you wish to be removed from the mailing list, or if the addressee is no longer employed by your organization, please notify PL/TSI, 29 Randolph Road, Hanscom AFB, MA 01731-3010. This will assist us in maintaining a current mailing list.

Do not return copies of this report unless contractual obligations or notices on a specific document requires that it be returned.

REPORT DOCUMENTATION PAGE

Form Approved
OMB No. 0704-0188

1. AGENCY USE ONLY *(Leave blank)*	2. REPORT DATE	3. REPORT TYPE AND DATES COVERED
	15 January 1997	Scientific Report No. 1

4. TITLE AND SUBTITLE
Thermospheric Density Variability and Forecast Model Development

5. FUNDING NUMBERS
PE 63707F
PR 4026 TA GL WU ME

Contract F19628-96-C-0019

6. AUTHOR(S)
Jeffrey M. Forbes
Timothy Fuller-Rowell

7. PERFORMING ORGANIZATION NAME(S) AND ADDRESS(ES)
University of Colorado
Department of Aerospace Engineering Sciences
Boulder, CO 80309

8. PERFORMING ORGANIZATION REPORT NUMBER

9. SPONSORING/MONITORING AGENCY NAME(S) AND ADDRESS(ES)
Phillips Laboratory
29 Randolph Road
Hanscom AFB, MA 01731-3010

Contract Manager: Frank Marcos/GPIM

10. SPONSORING/MONITORING AGENCY REPORT NUMBER

PL-TR-97-2016

11. SUPPLEMENTARY NOTES

12a. DISTRIBUTION AVAILABILITY STATEMENT

APPROVED FOR PUBLIC RELEASE; DISTRIBUTION UNLIMITED

12b. DISTRIBUTION CODE

13. ABSTRACT *(Maximum 200 words)*

Thermospheric densities derived from SETA-1, SETA-2 and SETA-3 accelerometer data, and cross-track winds from SETA-1, were analyzed to determine the nature of latitudinal structures at latitudes greater than 45 degrees. Distinct dependences on magnetic activity level, local time, hemisphere and season are revealed. Empirical models such as MSIS or J70 do not represent the observed high-latitude structures. The Coupled Thermosphere-Ionosphere Model (CTIM), however, is able to reproduce several of the salient high-latitude structures revealed in the SETA data, albeit usually at about half the amplitude.

14. SUBJECT TERMS		15. NUMBER OF PAGES
Thermospheric density Thermospheric winds	High latitudes	28
		16. PRICE CODE

17. SECURITY CLASSIFICATION OF REPORT	18. SECURITY CLASSIFICATION OF THIS PAGE	19. SECURITY CLASSIFICATION OF ABSTRACT	20. LIMITATION OF ABSTRACT
Unclassified	Unclassified	Unclassified	SAR

CONTENTS

TASK 1 - SETA DENSITY ANALYSES

1. Magnetic Storm Perturbations

The first of our data analysis efforts involved the SETA-1 data covering the March 22 - April 10, 1979, period. Color visualizations of the latitude vs. time development of the density response to varying geomagnetic activity were developed. A number of color plots have been produced in both geomagnetic and geographic coordinates, for both density and cross-track wind. These figures have been provided to Mr. Marcos at Phillips Laboratory. These visualizations have enabled us to evaluate optimum periods to run the CTIM model so that the SETA densities can be used as means of model validation. These efforts are described further in the **MODEL DEVELOPMENT** section.

2. High-Latitude Structures: SETA-1

Recognizing that the largest data/model discrepancies occur at high latitudes; and also that the existence of "density cells" (sometimes consisting of *depressions* in density during high magnetic activity – a feature not predicted by any empirical models) seems to be generally accepted; we have initiated an investigation to see if such features can be uncovered in the SETA data in a *statistical sense*. We have begun this work on the SETA-1 data base, since both densities and winds are available during this period. Figures 1-6 summarize these results. Note that density and wind plots are available for both day (N. Hemis. and S. Hemis.) and night (N. Hemis. only). These figures are shown in geomagnetic coordinates, but they are also available in geographic coordinates. The data are normalized to 45 degrees latitude; densities are normalized to unity – and winds represent the winds with the value at 45 degrees subtracted; therefore, the densities are normalized to unity at 45 degrees, and the winds to zero at these latitudes. The purpose of this normalization is to examine only the *latitude structure* poleward of 45°. This will allow future studies to mix different seasons and levels of solar activity with minimum contamination.

These figures reveal a number of interesting features which are not completely understood. In Figure 1, the latitude structure is distinctly different for the 3 Kp levels, and a "depression" or "cell" seems to be visible for intermediate Kp levels. The daytime winds (Figure 2) do not reveal much dependence on Kp. In Figure 3, the highest Kp curve shows the lowest density compared to 45°, again suggestive of a cell. On the nightside, the winds (Figure 4) increase in intensity with magnetic activity; daytime densities in the S. Hemis. all show evidence of a depression at high latitudes (Figure 5). And, in contrast to the N. Hemis. wind results, the daytime winds in the S. Hemis. (Figure 6) show a distinct inrease in intensity with Kp. It is our hope that by comparison of these results with climatological results from CTIM, we will begin to understand the physical mechanisms underlying these

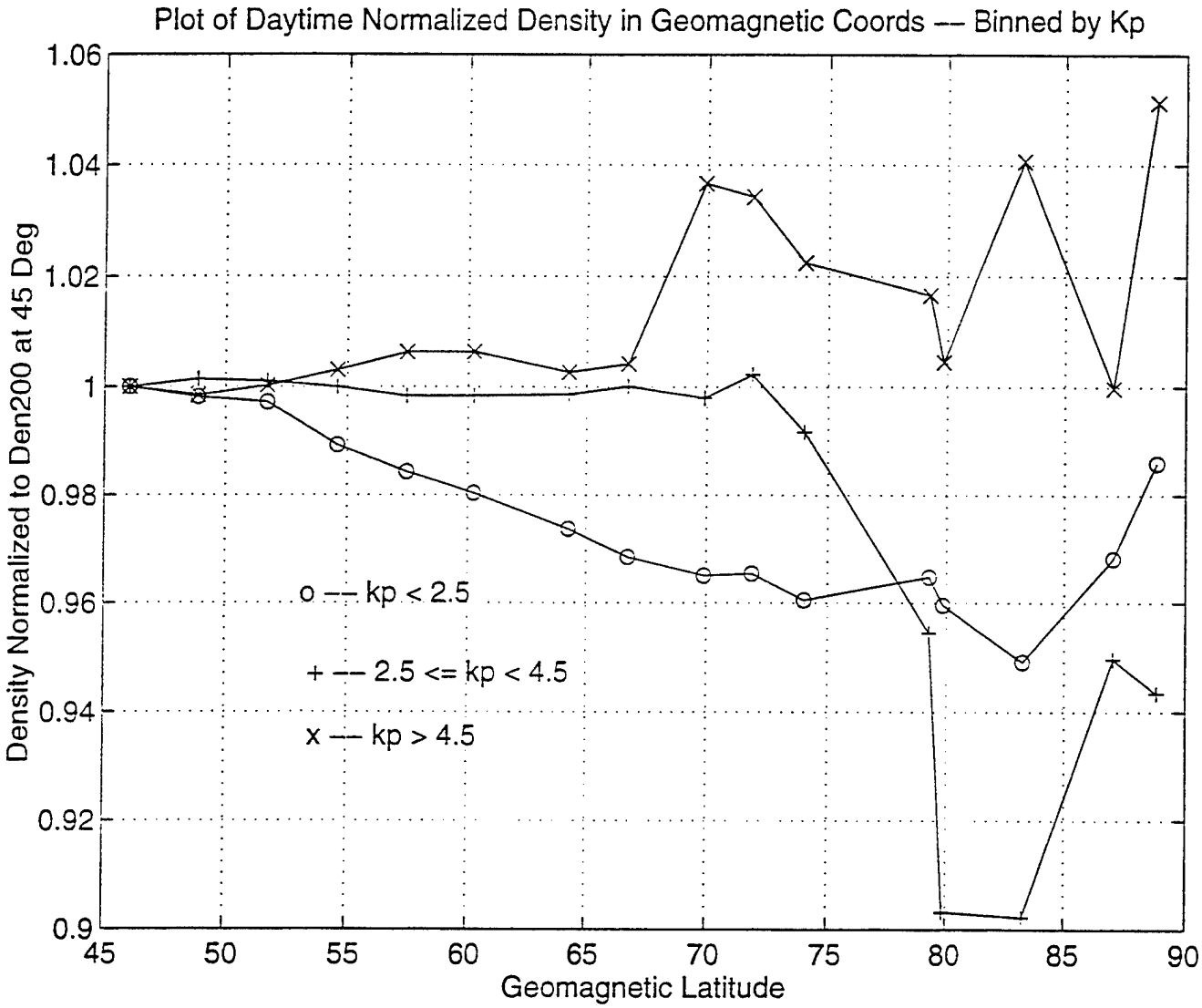
Plot of Daytime Normalized Density in Geomagnetic Coords -- Binned by Kp
Density Normalized to Den200 at 45 Deg
Geomagnetic Latitude
1.06
1.04
1.02
1
0.98
0.96
0.94
0.92
0.9
45
50
55
60
65
70
75
80
85
90
o -- kp < 2.5
+ -- 2.5 <= kp < 4.5
x -- kp > 4.5

Figure 1

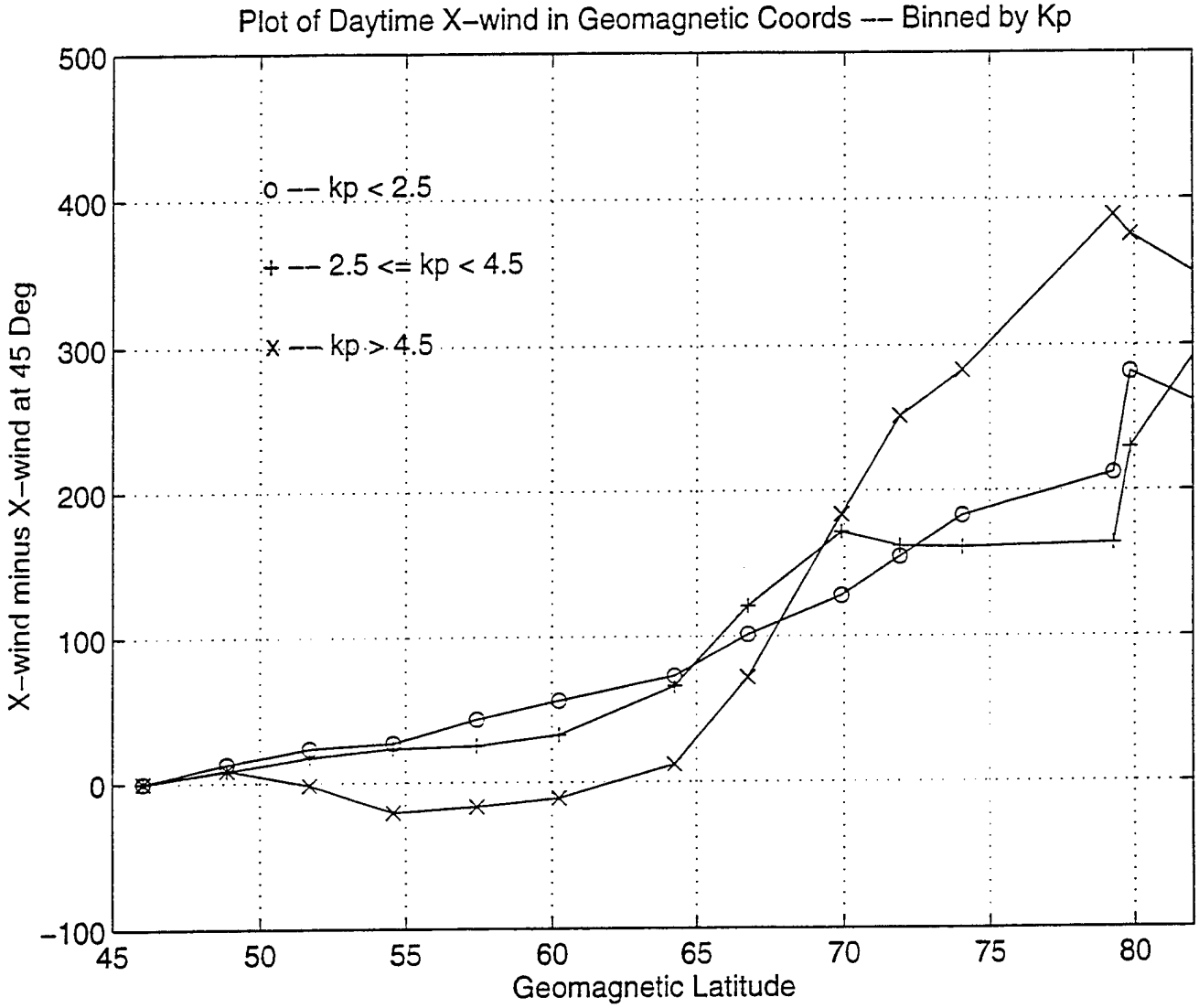
Plot of Daytime X–wind in Geomagnetic Coords –– Binned by Kp
o –– kp < 2.5
+ –– 2.5 <= kp < 4.5
x –– kp > 4.5
X–wind minus X–wind at 45 Deg
Geomagnetic Latitude
500
400
300
200
100
0
−100
45
50
55
60
65
70
75
80

Figure 2

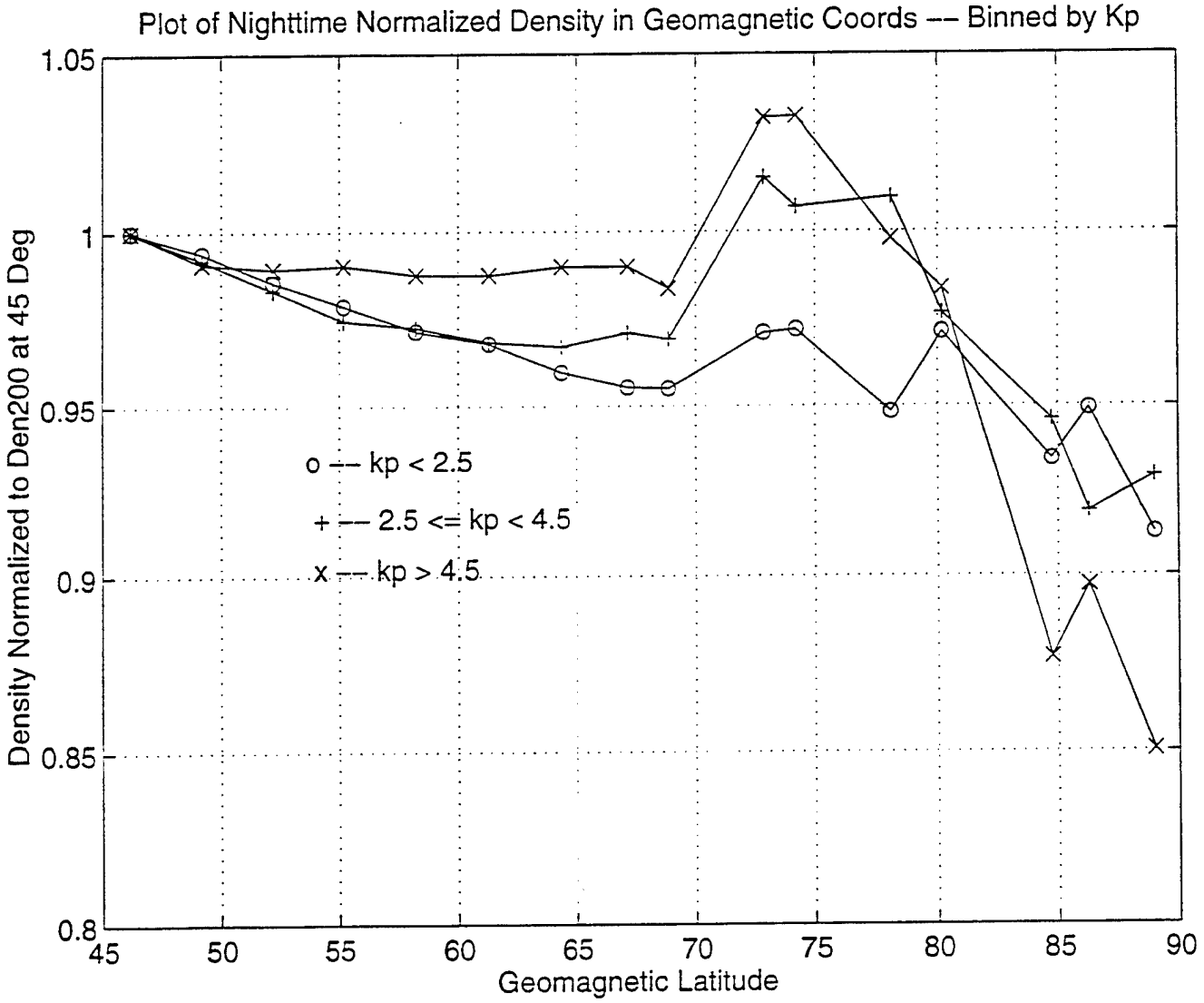
Plot of Nighttime Normalized Density in Geomagnetic Coords --- Binned by Kp
Density Normalized to Den200 at 45 Deg
Geomagnetic Latitude
1.05
1
0.95
0.9
0.85
0.8
45
50
55
60
65
70
75
80
85
90
o --- kp < 2.5
+ --- 2.5 <= kp < 4.5
x --- kp > 4.5

Figure 3

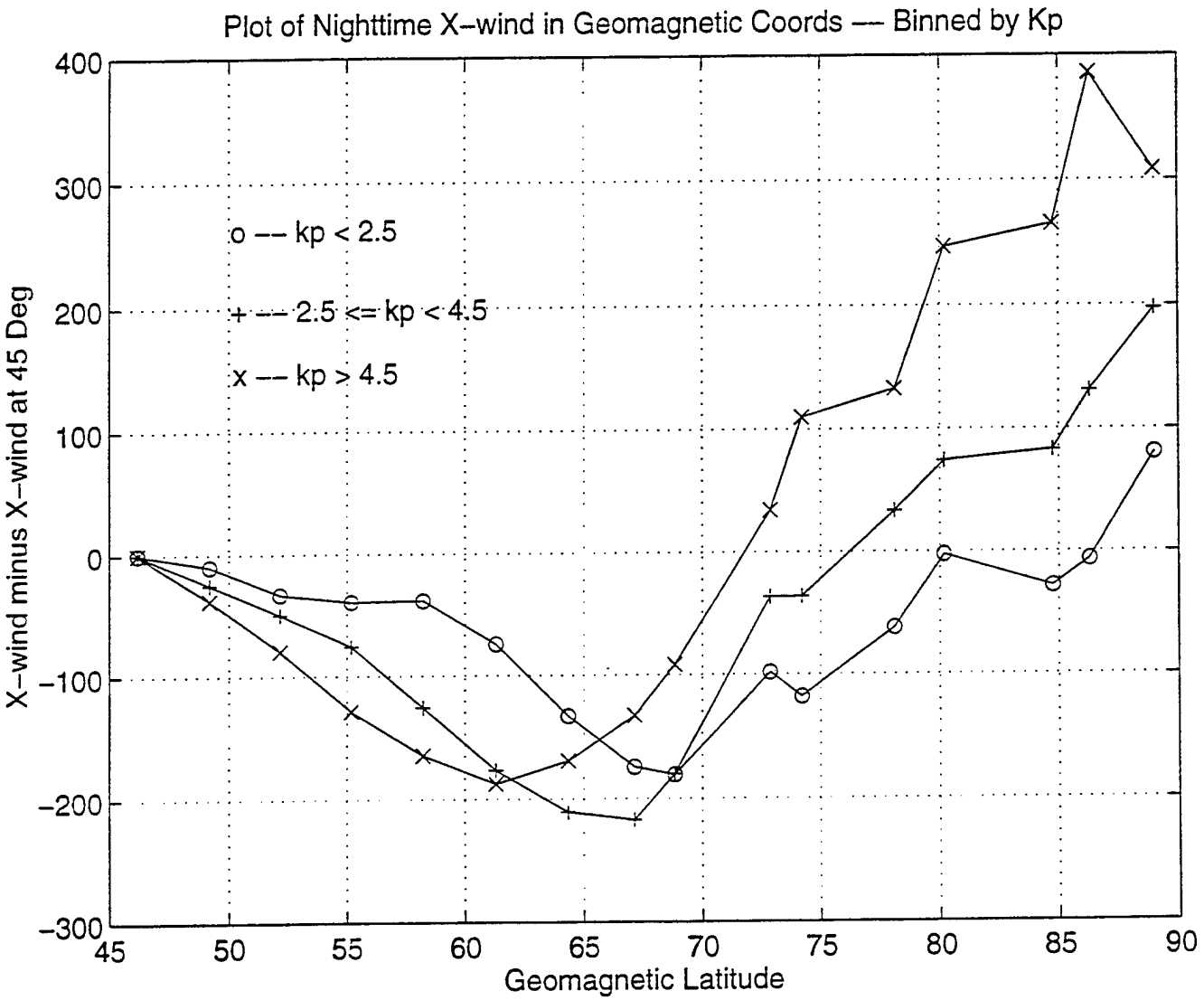
Plot of Nighttime X-wind in Geomagnetic Coords — Binned by Kp
o — kp < 2.5
+ — 2.5 <= kp < 4.5
x — kp > 4.5
X-wind minus X-wind at 45 Deg
Geomagnetic Latitude
400
300
200
100
0
-100
-200
-300
45
50
55
60
65
70
75
80
85
90

Figure 4

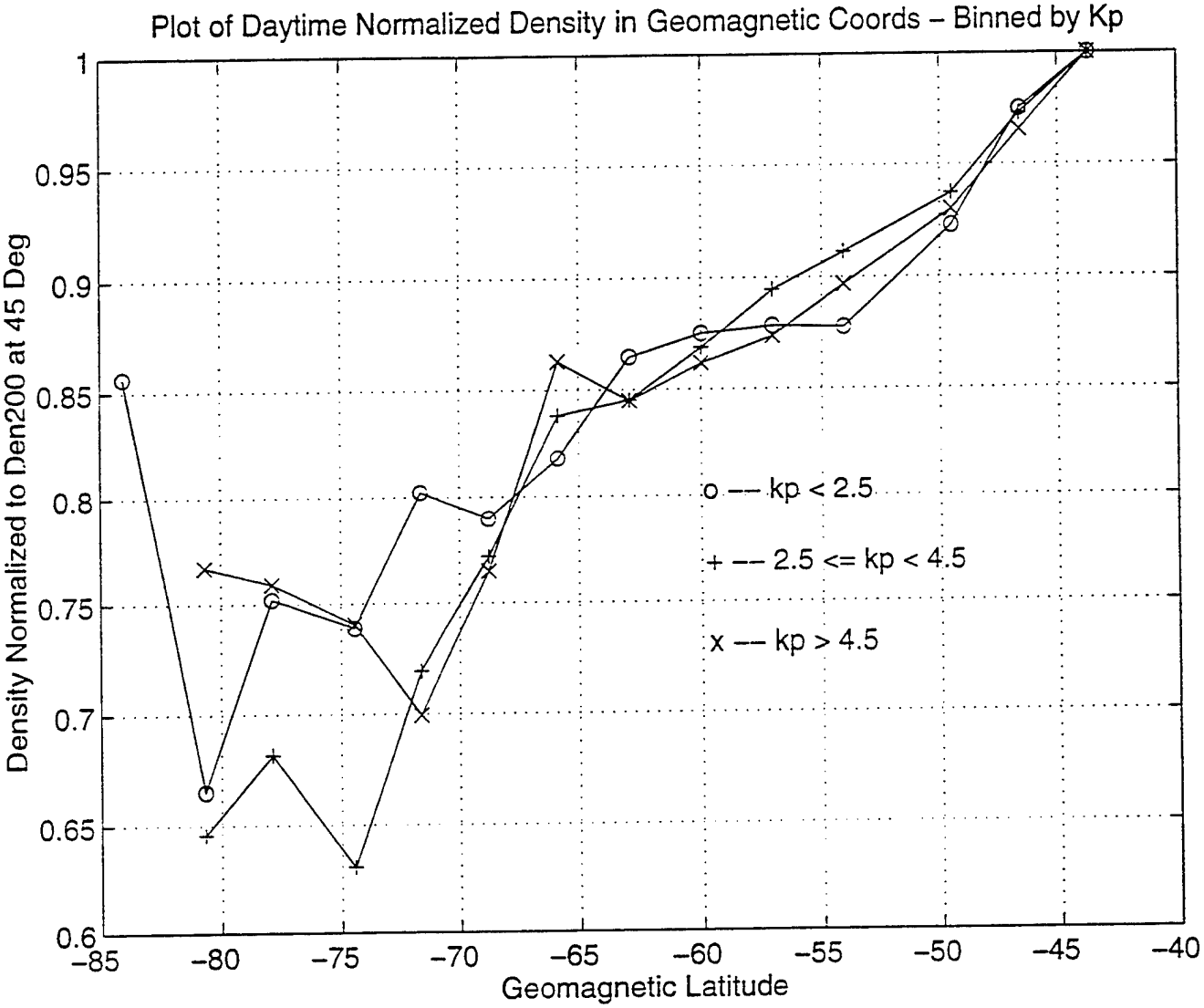
Plot of Daytime Normalized Density in Geomagnetic Coords – Binned by Kp
Density Normalized to Den200 at 45 Deg
Geomagnetic Latitude
1
0.95
0.9
0.85
0.8
0.75
0.7
0.65
0.6
−85
−80
−75
−70
−65
−60
−55
−50
−45
−40
o — kp < 2.5
+ — 2.5 <= kp < 4.5
x — kp > 4.5

Figure 5

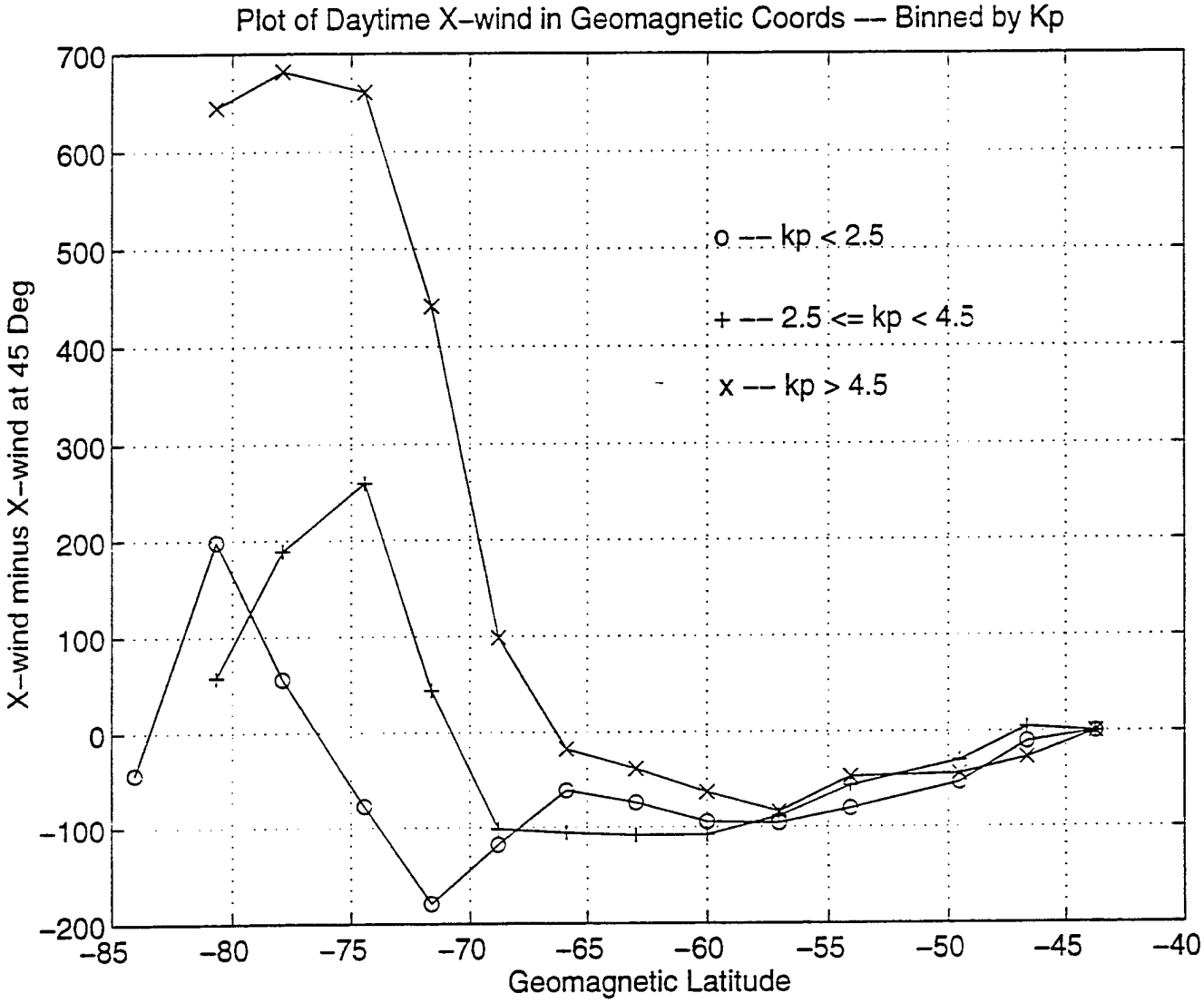
Plot of Daytime X-wind in Geomagnetic Coords --- Binned by Kp
X-wind minus X-wind at 45 Deg
Geomagnetic Latitude
o --- kp < 2.5
+ --- 2.5 <= kp < 4.5
x --- kp > 4.5
700
600
500
400
300
200
100
0
-100
-200
-85
-80
-75
-70
-65
-60
-55
-50
-45
-40

Figure 6

structures, and to incorporate them into future predictive capabilities. This has indeed been performed with the more extensive SETA-2 and SETA-3 data sets, as described in the following.

3. High-Latitude Structures: SETA-2 and SETA-3

Based on our reasonable success delineating significant high-latitude structures using the SETA-1 data (March/April, 1979), and considering the potential contribution of high-latitude structures to the 15% barrier in model/data discrepancies, this area has been further pursued through analyses of the SETA-2 and SETA-3 data sets during 1982 and 1983, respectively. For ALL of the data available for these two missions, we have binned the densities into seasonal and Kp bins, as indicated in the attached table. The seasons are summer, winter, equinox, defined respectively according to the months JJA, NDJ, MASO for the N. Hemisphere, and with a 6-month shift for the S. Hemisphere. Note that there are on the order of 600-800 orbits averaged for low magnetic activity, 300-500 for moderate activity, and roughly 100-200 orbits averaged for active magnetic conditions.

Figures 7, 8, 9 delineate these results for the SETA data; Figures 10 and 11 for the corresponding MSIS model results, where point-by-point calculations and binning are identical to those for the SETA data points; and Figures 12 and 13 provide climatological results from the Jacchia 1970 (J70) model corresponding to July and December, 1983 conditions. Note that all densities are normalized to a value of 1.0 at 45 degrees latitude; this was done so that density structures from various solar activity levels could be averaged meaningfully. We note that the SETA data reveal some clear latitude and Kp dependences that the MSIS and J70 models do not. These unmodeled variations could be potentially important for future density forecasting efforts.

We have begun to investigate the sources of the above variations by running the CTIM model for similar conditions, and preparing the same plots. These results are depicted in Figures 14 and 15 for June and December CTIM runs for similar solar conditions, and over the same range of geomagnetic conditions. We note that in many cases the *sense* of the latitude variation *and* its dependence on Kp are similar to those exhibited by the SETA data, although less pronounced. The presence of these variations allows us to examine the CTIM model to uncover and physical mechanisms underlying the effects; moreover, once this is done, it may then be possible to "correct" CTIM to better reproduce the density measurements – this type of process is at the heart of our validation efforts.

One must be cognizant that some part of the SETA variations is due to in-track wind effects on the measured accelerations, which cannot be separated from the density-induced accelerations. The CTIM model has been used to provide a check on this issue. Figures 16 and 17 are the same as Figures 14 and 15, except that the in-track projection of the CTIM

Table 1

Orbit # / Season	Kp <= 3	3< Kp <5	Kp >=5
Winter	705	438	110
Transition	814	494	213
Summer	573	264	138

Winter: Nov., 1982, Jan.,Feb., Dec., 1983

Transition: Sep., Oct., 1982, Sep., Oct., Mar., 1983

Summer: Jun.,Jul.,1982, Jul., Aug., 1983

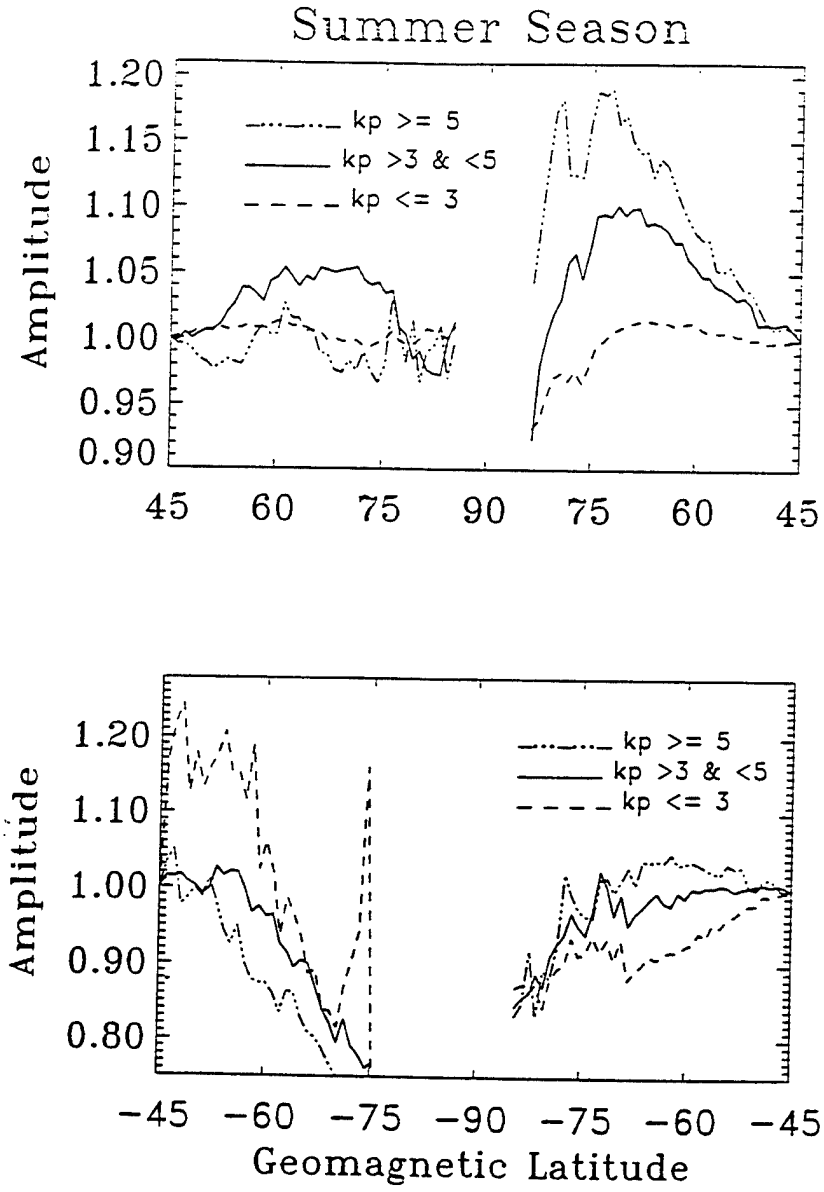
Summer Season
Amplitude
1.20
1.15
1.10
1.05
1.00
0.95
0.90
kp >= 5
kp >3 & <5
kp <= 3
45
60
75
90
75
60
45
Amplitude
1.20
1.10
1.00
0.90
0.80
kp >= 5
kp >3 & <5
kp <= 3
-45
-60
-75
-90
-75
-60
-45
Geomagnetic Latitude

Figure 7

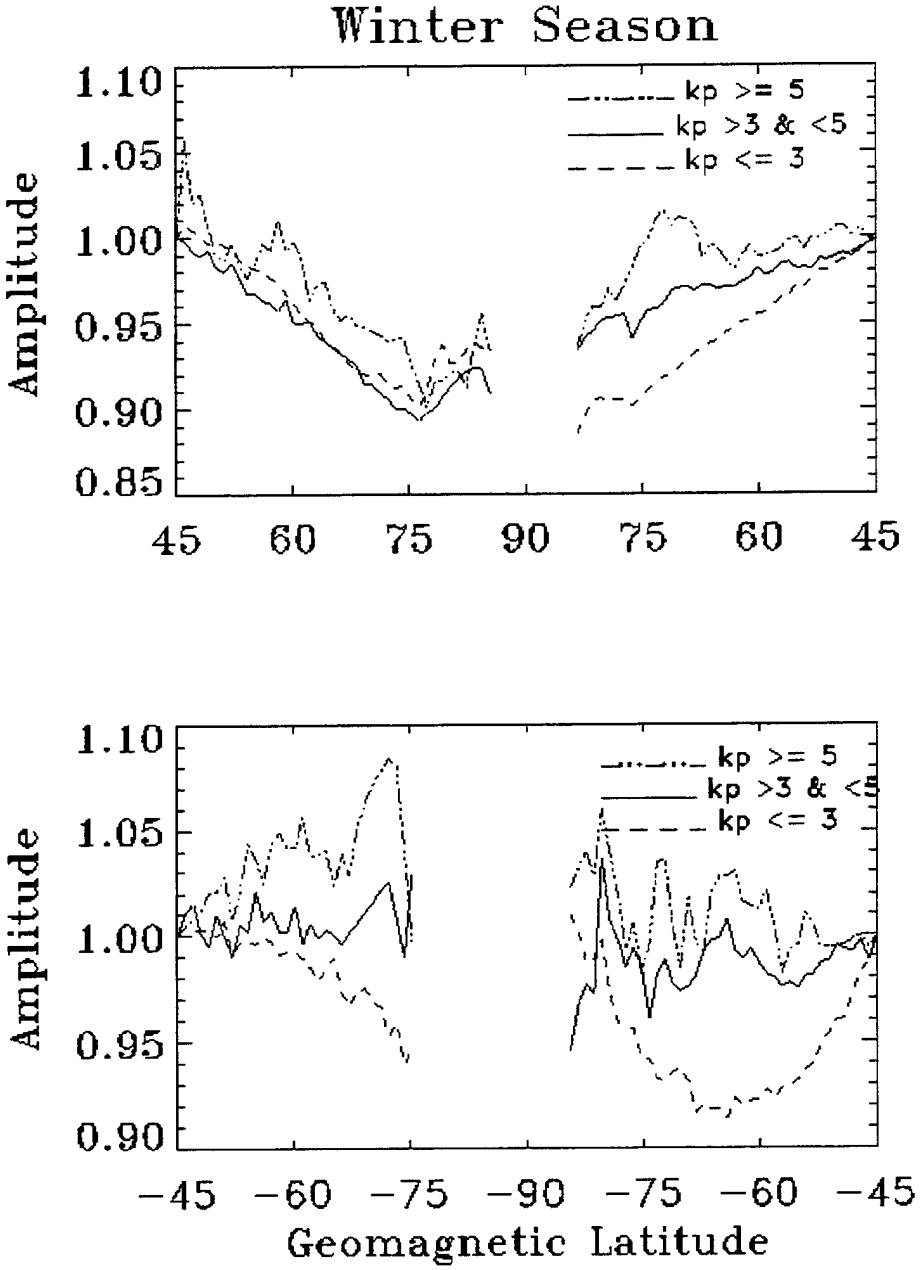
Winter Season
Amplitude
1.10
1.05
1.00
0.95
0.90
0.85
kp >= 5
kp >3 & <5
kp <= 3
45
60
75
90
75
60
45
Amplitude
1.10
1.05
1.00
0.95
0.90
kp >= 5
kp >3 & <5
kp <= 3
−45
−60
−75
−90
−75
−60
−45
Geomagnetic Latitude

Figure 8

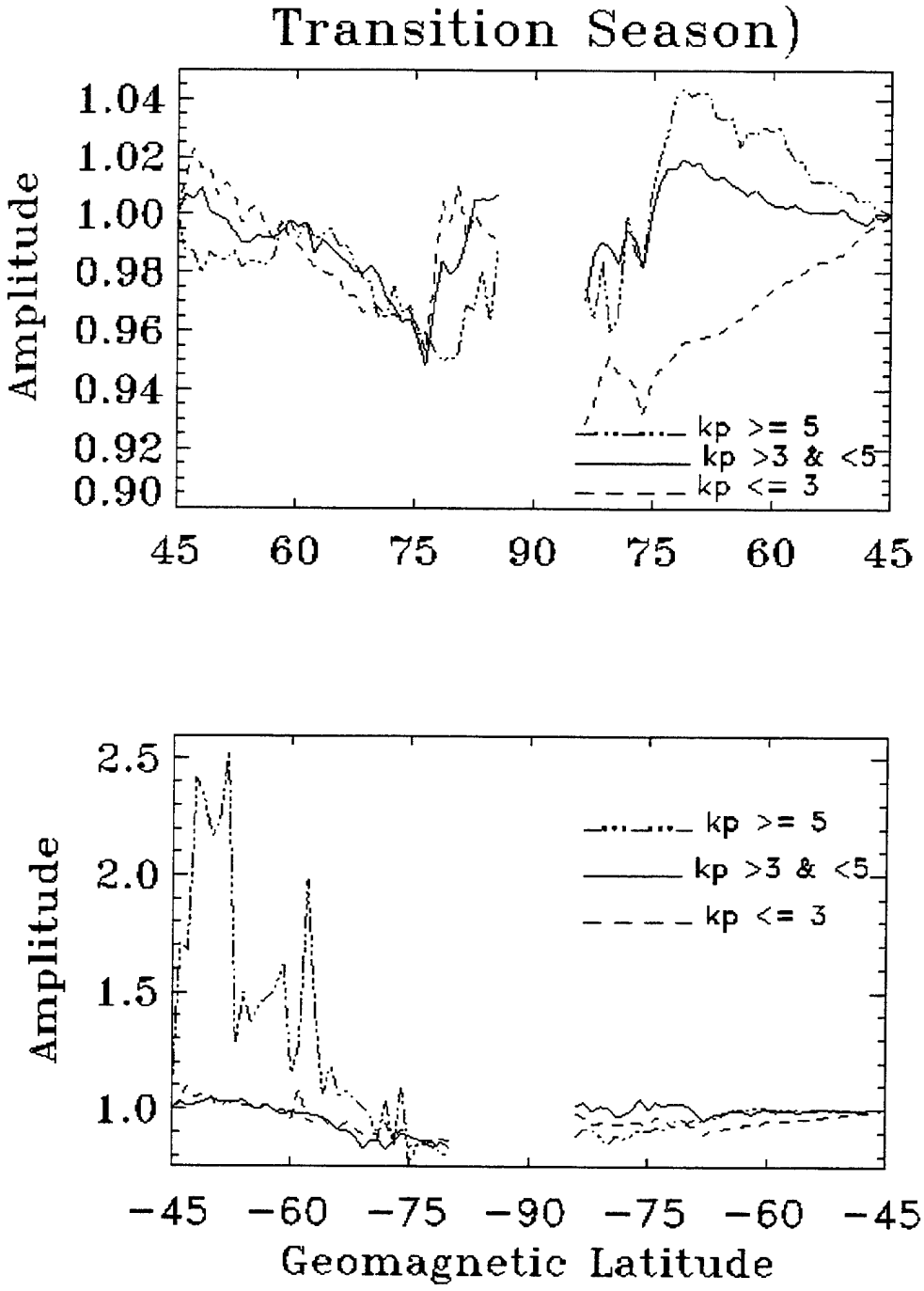
Transition Season)
Amplitude
1.04
1.02
1.00
0.98
0.96
0.94
0.92
0.90
45
60
75
90
75
60
45
kp >= 5
kp >3 & <5
kp <= 3
Amplitude
2.5
2.0
1.5
1.0
kp >= 5
kp >3 & <5
kp <= 3
-45
-60
-75
-90
-75
-60
-45
Geomagnetic Latitude

Figure 9

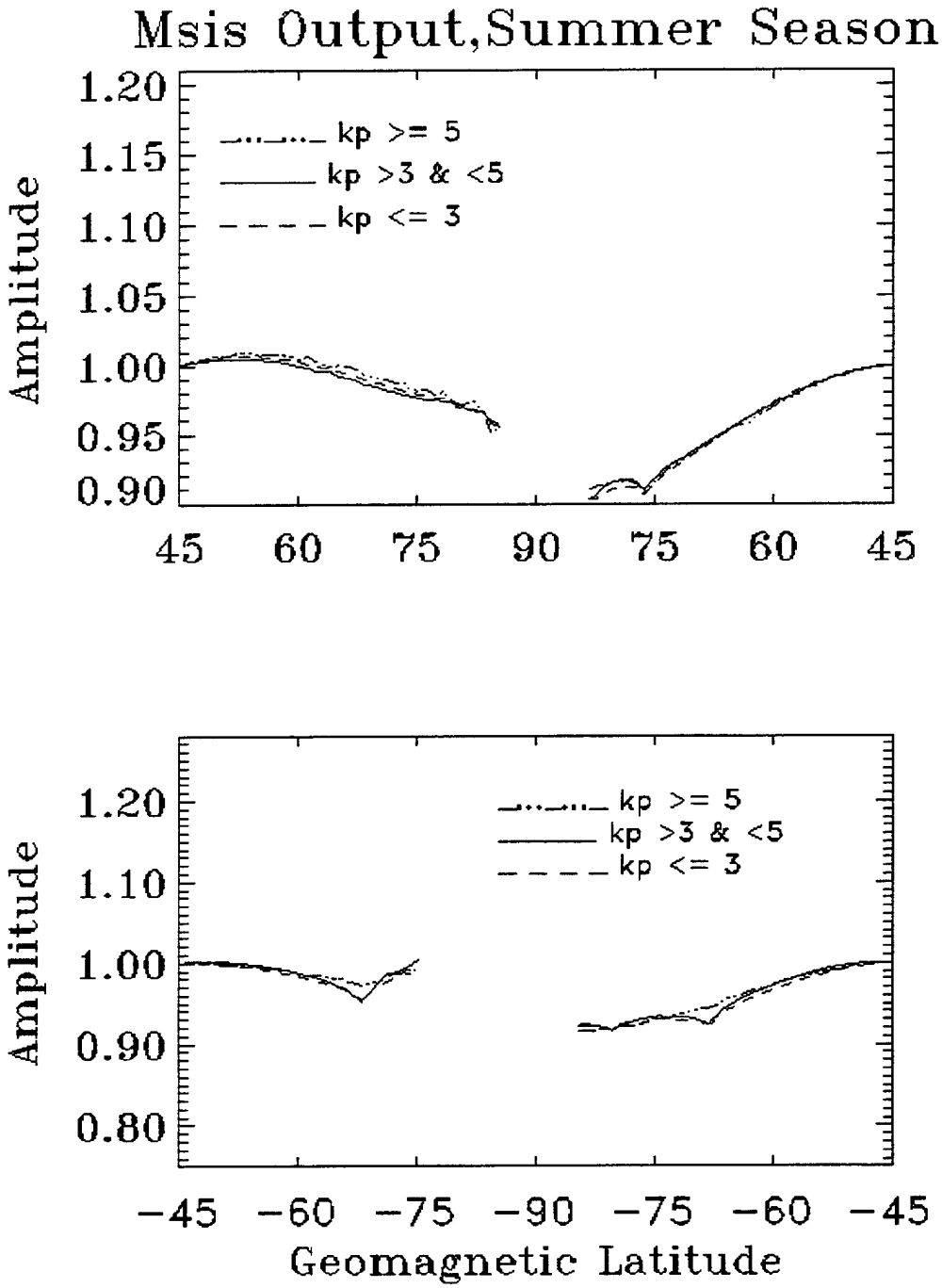
Msis Output,Summer Season
Amplitude
1.20
1.15
1.10
1.05
1.00
0.95
0.90
kp >= 5
kp >3 & <5
kp <= 3
45
60
75
90
75
60
45
Amplitude
1.20
1.10
1.00
0.90
0.80
kp >= 5
kp >3 & <5
kp <= 3
-45
-60
-75
-90
-75
-60
-45
Geomagnetic Latitude

Figure 10

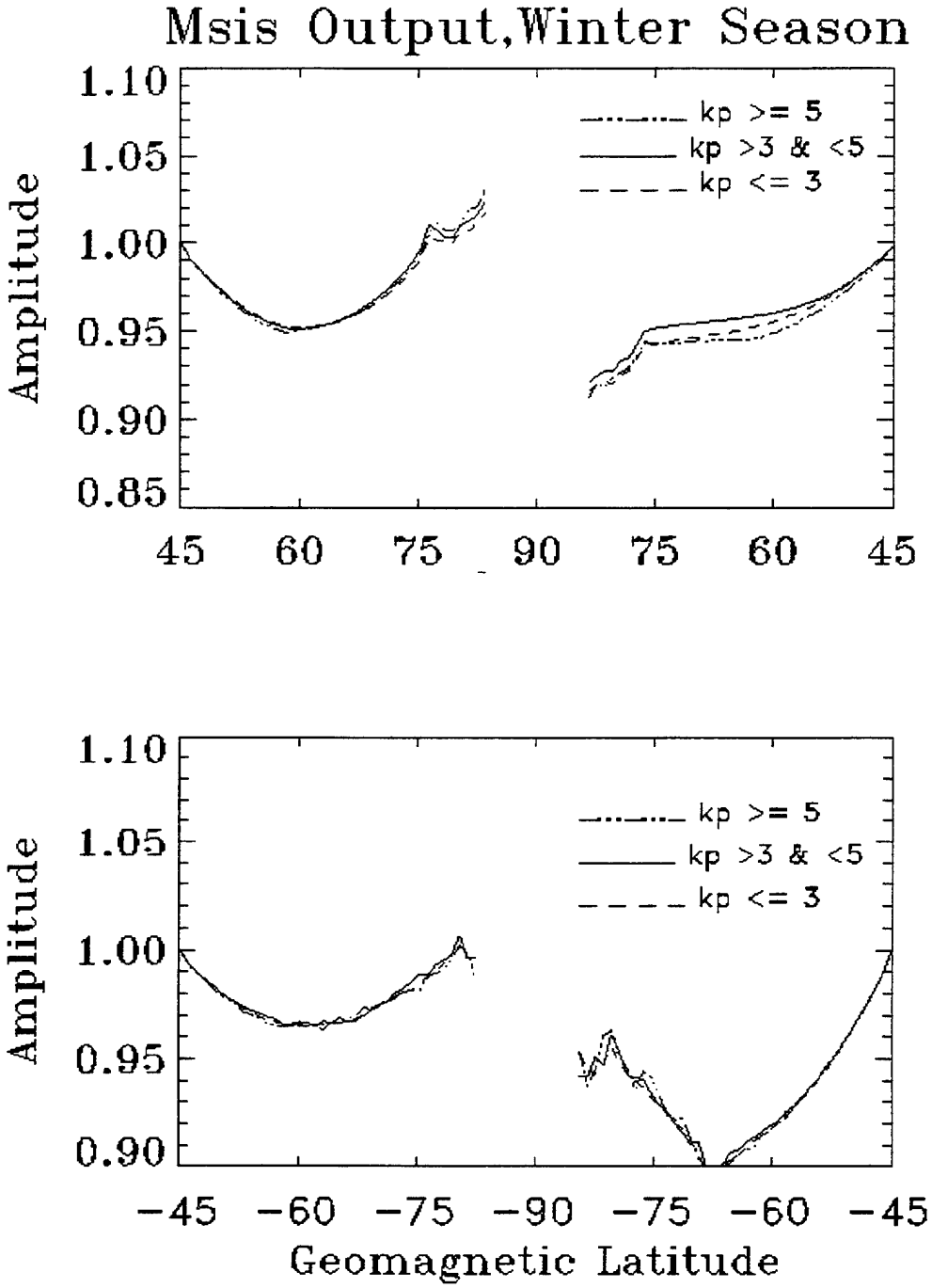
Msis Output,Winter Season
Amplitude
1.10
1.05
1.00
0.95
0.90
0.85
kp >= 5
kp >3 & <5
kp <= 3
45
60
75
90
75
60
45
Amplitude
1.10
1.05
1.00
0.95
0.90
kp >= 5
kp >3 & <5
kp <= 3
-45
-60
-75
-90
-75
-60
-45
Geomagnetic Latitude

Figure 11

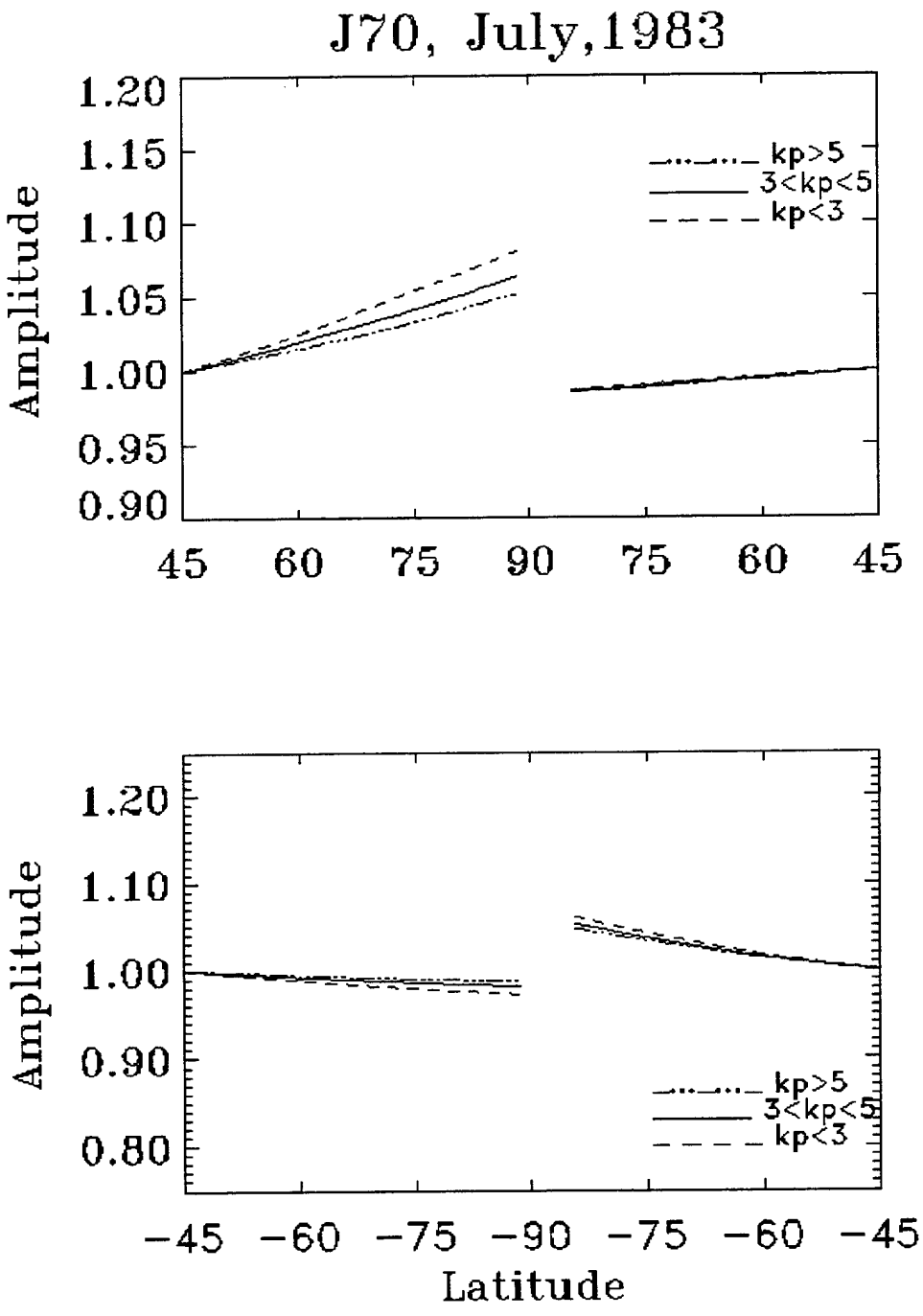
J70, July,1983
Amplitude
1.20
1.15
1.10
1.05
1.00
0.95
0.90
45 60 75 90 75 60 45
kp>5
3<kp<5
kp<3
Amplitude
1.20
1.10
1.00
0.90
0.80
−45 −60 −75 −90 −75 −60 −45
Latitude
kp>5
3<kp<5
kp<3

Figure 12

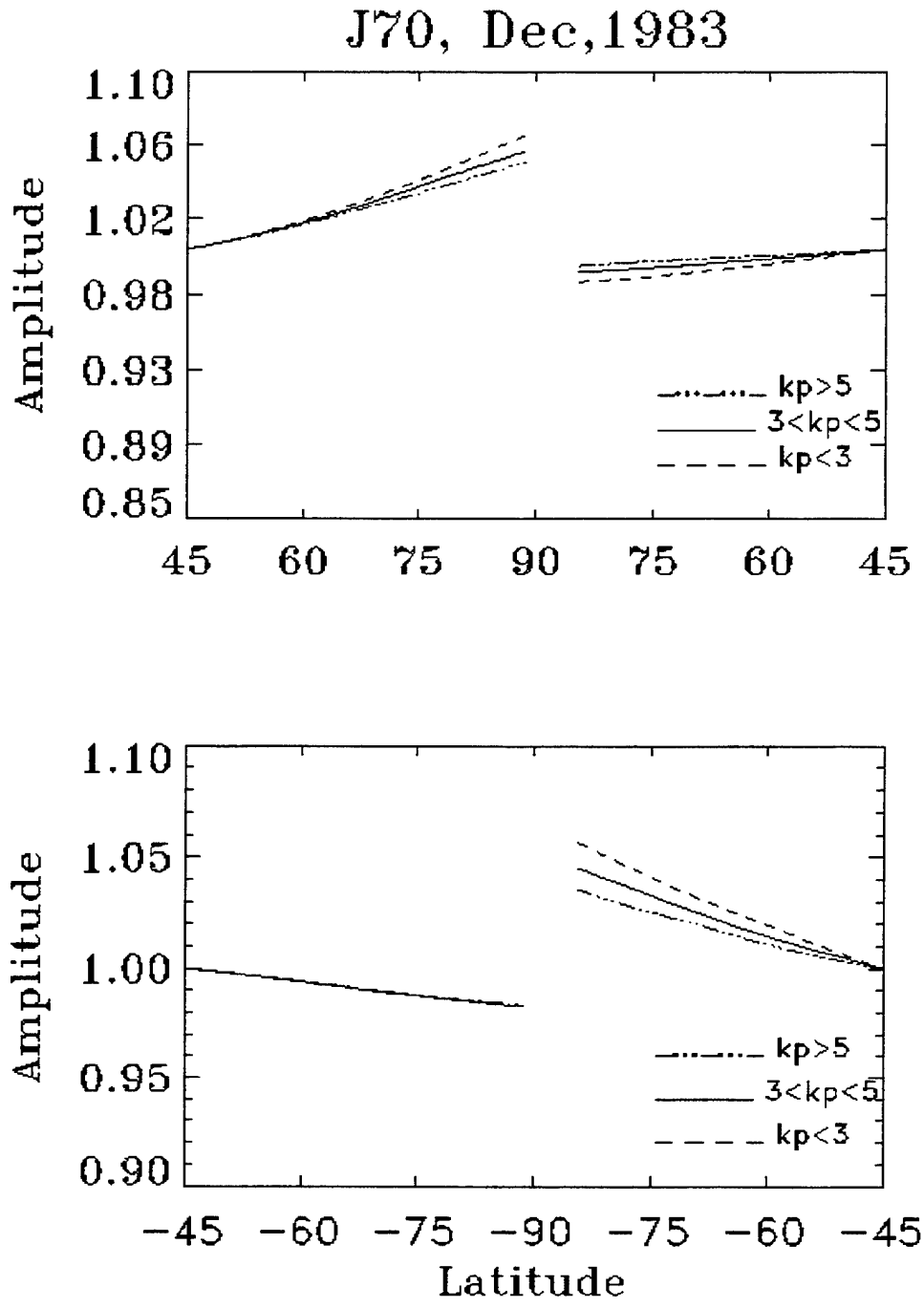
J70, Dec,1983
Amplitude
1.10
1.06
1.02
0.98
0.93
0.89
0.85
45
60
75
90
75
60
45
kp>5
3<kp<5
kp<3
Amplitude
1.10
1.05
1.00
0.95
0.90
−45
−60
−75
−90
−75
−60
−45
Latitude
kp>5
3<kp<5
kp<3

Figure 13

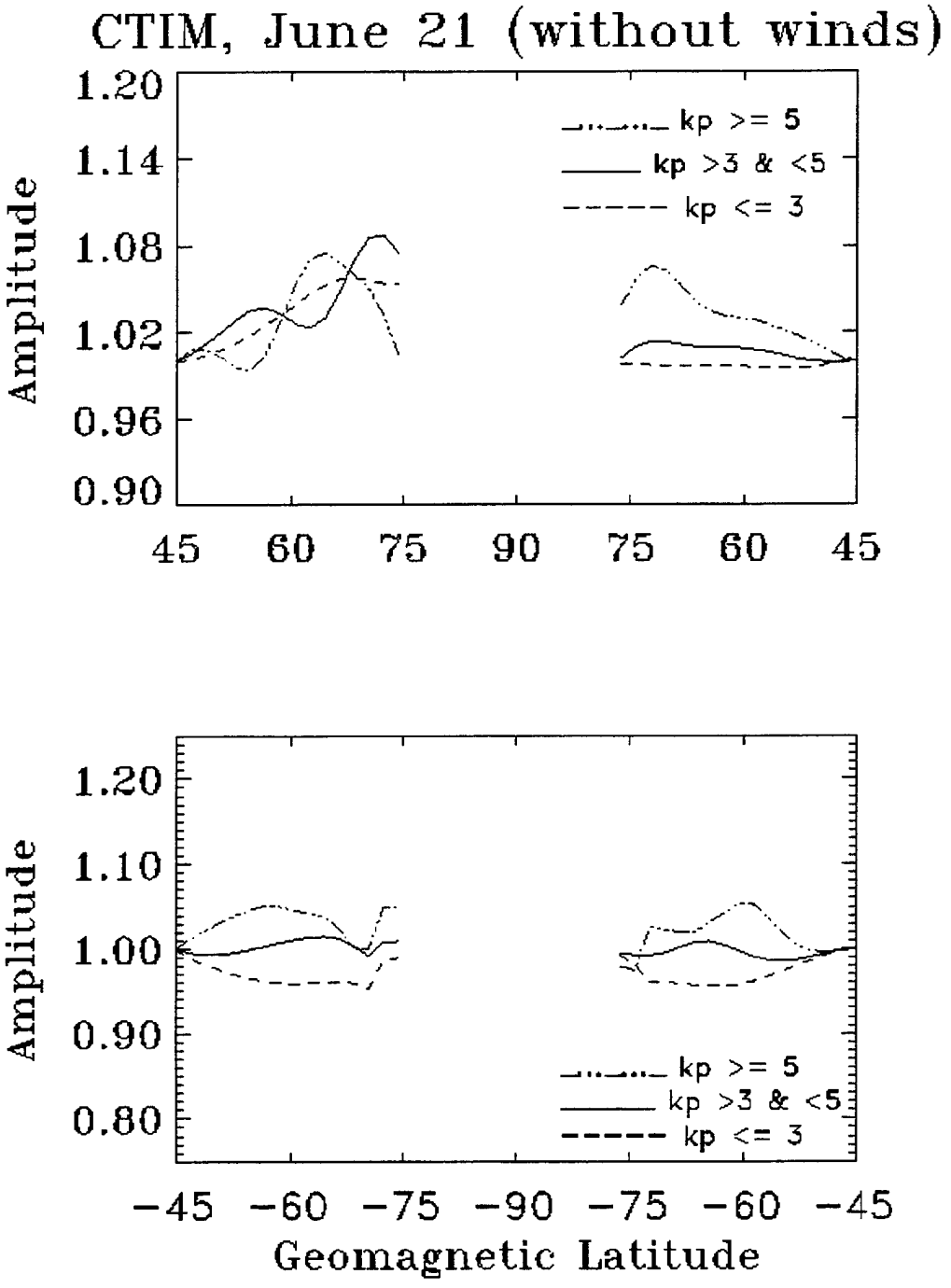
CTIM, June 21 (without winds)
Amplitude
1.20
1.14
1.08
1.02
0.96
0.90
kp >= 5
kp >3 & <5
kp <= 3
45 60 75 90 75 60 45
Amplitude
1.20
1.10
1.00
0.90
0.80
kp >= 5
kp >3 & <5
kp <= 3
-45 -60 -75 -90 -75 -60 -45
Geomagnetic Latitude

Figure 14

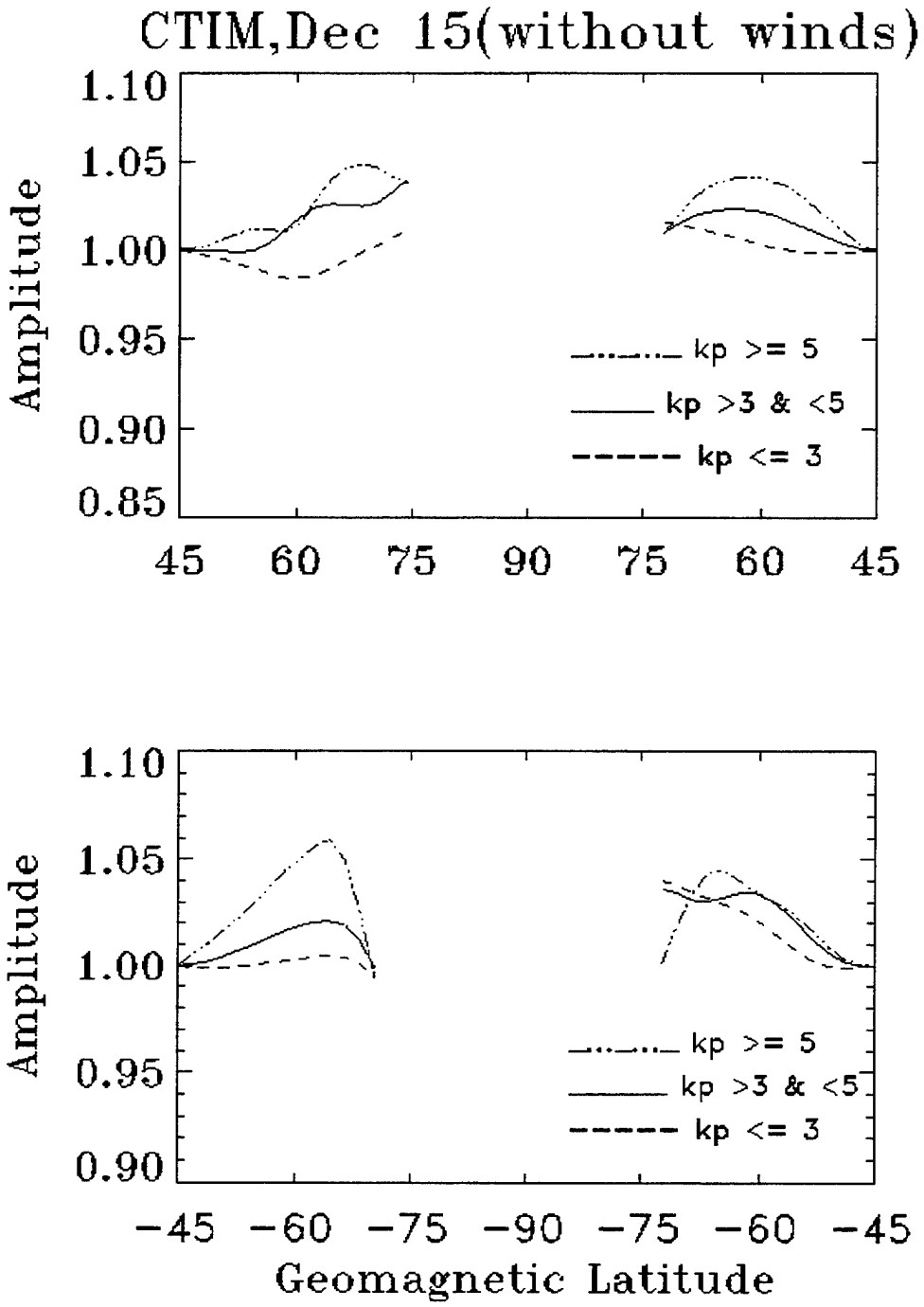
CTIM,Dec 15(without winds)
Amplitude
1.10
1.05
1.00
0.95
0.90
0.85
45 60 75 90 75 60 45
kp >= 5
kp >3 & <5
kp <= 3
Amplitude
1.10
1.05
1.00
0.95
0.90
-45 -60 -75 -90 -75 -60 -45
Geomagnetic Latitude
kp >= 5
kp >3 & <5
kp <= 3

Figure 15

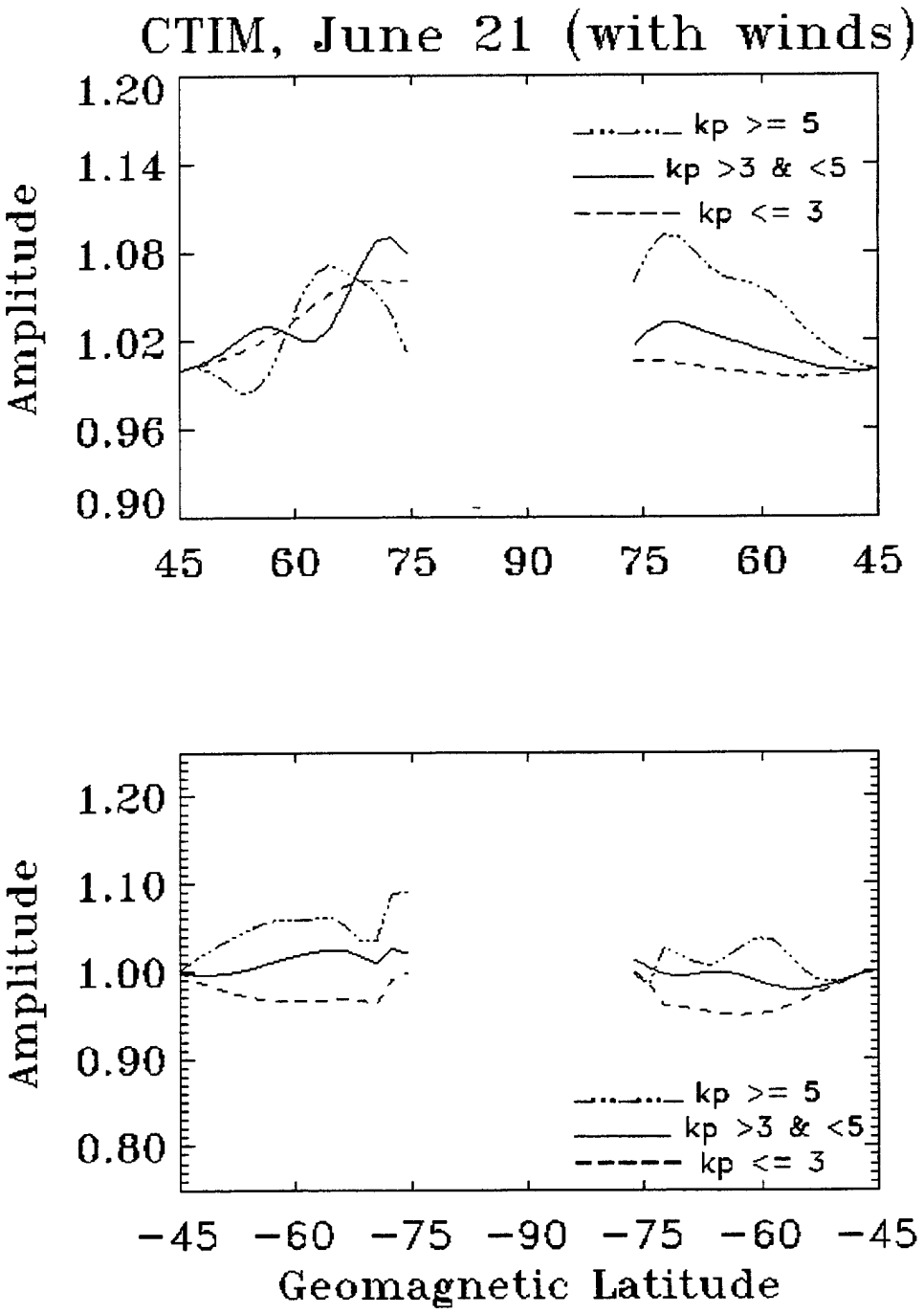
CTIM, June 21 (with winds)
Amplitude
1.20
1.14
1.08
1.02
0.96
0.90
kp >= 5
kp >3 & <5
kp <= 3
45 60 75 90 75 60 45
Amplitude
1.20
1.10
1.00
0.90
0.80
kp >= 5
kp >3 & <5
kp <= 3
-45 -60 -75 -90 -75 -60 -45
Geomagnetic Latitude

Figure 16

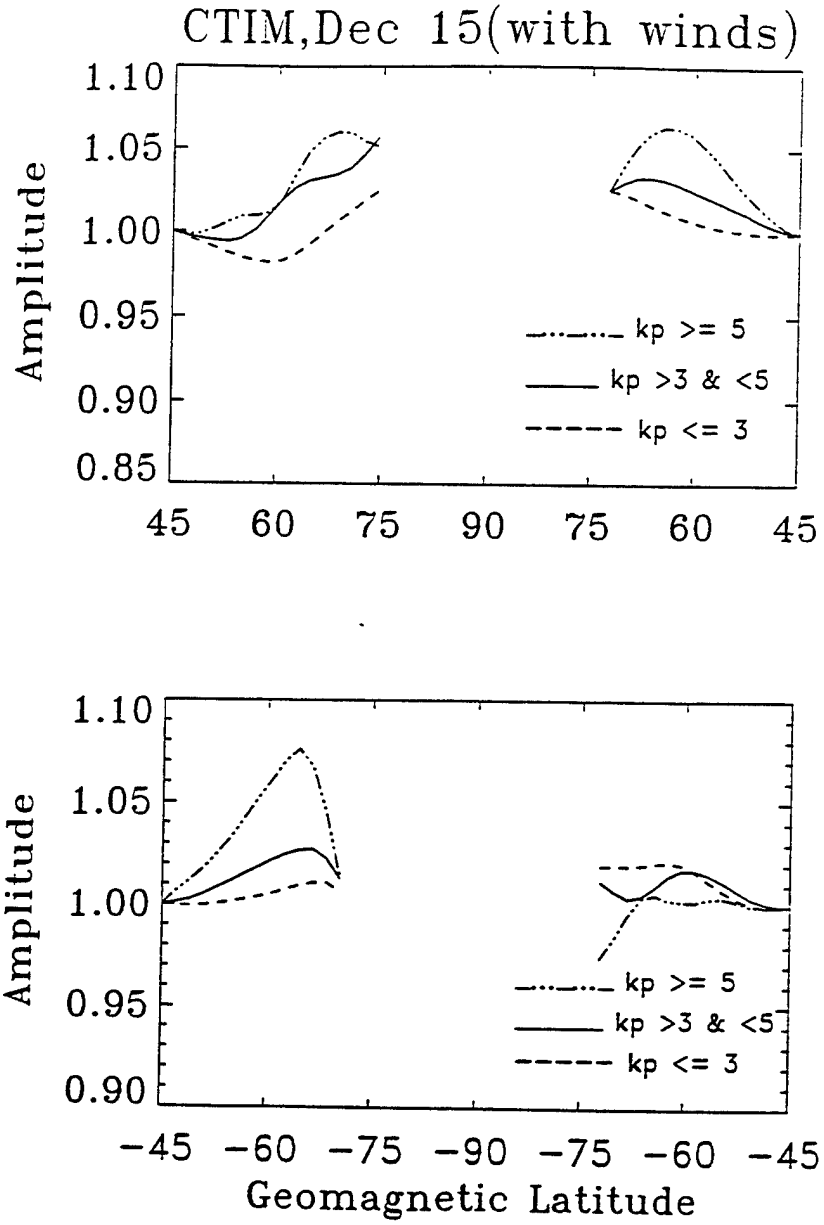
CTIM,Dec 15(with winds)
Amplitude
1.10
1.05
1.00
0.95
0.90
0.85
45 60 75 90 75 60 45
kp >= 5
kp >3 & <5
kp <= 3
Amplitude
1.10
1.05
1.00
0.95
0.90
-45 -60 -75 -90 -75 -60 -45
Geomagnetic Latitude
kp >= 5
kp >3 & <5
kp <= 3

Figure 17

wind vectors have been included in the depicted densities. It is noted that there is some small tendency for the winds to accentuate the structures noted above, but that these are relatively small. This suggests that the densities inferred from SETA, and their latitudinal and Kp variations, are correct. However, we plan to perform a second-level check on CTIM winds during the SETA-1 interval to ascertain whether we might have underestimated the wind correction effect.

MODEL DEVELOPMENT

1. Validation Process for Atmospheric Density and Ionospheric Change

During the first year we have focused on a four day period (March 20-23, 1979) during which two geomagnetic disturbances occurred. The goal was to determine the cause of the plateau in the accuracy of model prediction of atmospheric density for the last 25 years. The variance between model and atmospheric density data has remained the same over this time inspite of the increase in understanding and modelling of upper atmosphere processes. We have simulated this four-day period forcing the model in the simplest possible way: using statistical patterns of auroral precipitation and convective electric field. The magnitude of the statistical patterns were defined by the auroral hemispheric power index derived from TIROS/NOAA observation of auroral particle precipitation. This is our standard automated process for performing a simulation of a particular interval, providing the power index is available.

The statistical analysis revealed, as we expected, a similar variance for the model/data comparison as can be found by using standard empirical models such as MSIS and Jacchia. There are two reasons for the results. First, the magnitude of the driving force is not correctly specified, and second the particular time sequence on the pulses of energy input is not timed correctly.

The first problem can be seen by examining a series of orbits following the first injection of energy. The data clearly shows the orbit passing through a density hole, possibly driven by divergence of the neutral dynamics rather than heat input, but this is yet to be verified. Using statistical magnitudes for the magnetospheric sources, the depth of these density holes are too shallow. Experience with alternative forcing functions have shown that a much stronger electric field magnitude is required to produce the observed depth of the holes.

The second problem is related to the first. Examination of another sequences of orbits from the SETA data reveal clear propagation of energy equatorward following an energy injection. The sequence is repeatable in the data with first, a density increase seen at high latitudes, followed by a density bulge at midlatitude and low latitude on subsequent

orbits. The propagation is consistent with large scale internal gravity waves. In the numerical simulation the same wave features are evident but with reduced magnitude and with incorrect timing sequence.

The increase in variance in the data during these two types of density perturbations is clearly seen in the data. It is clear that the increase in variance is caused partly by these two distinct processes, but it is not clear if they are the only processes that cause the problem. To address this question the next step is to try to match the magnitude and time sequence of the magnetospheric drivers to the observations. This task is currently in progress. The other cause for the model/data variance is the spatial distribution of the driving sources. If a density hole can be simulated, but is not in the correct location, it indicates a correct magnitude of the driving electric field and momentum source but an incorrect spatial distribution. These questions will be addressed in the following year.

An alternative approach is to validate the model by comparing with the ionospheric response. Ionosonde data for this period was analyzed to quantify the magnitude of the midlatitude negative phase and its regional dependence. This dataset is currently under scrutiny to determine if it can be used to further quantify the model input fields.

2. Semi-Annual Density Variation

On the longer time-scales one of the largest differences between empirical models and density data is the magnitude of the semiannual variation. This variation is imposed within the empirical models although no mechanism had been accepted.

One of the focii for the model development during the first year has been analysis of the semi-annual variations of atmospheric density as simulated by the physically-based model. Observations have demonstrated a significantly larger density at equinox as measured at a fixed satellite altitude. Only part of this increase in amplitude can be attributed to thermal expansion from higher globally-averaged temperature at equinox. A requirement of the model is to be able to reproduce the semi-annual variation. If such a variation is not simulated by the model as a natural phenomena, then it will be necessary to impose such a variation artifically. No physically-based model has been able to demonstate such a variation.

Analysis of solstice and equinox model simulations under identical solar flux reveals a substantial semiannual variation, with an amplitude similar to observations. Part of the change results from greater globally-averaged heating at high latitudes from Joule heating. The implication is that the sum of Joule heating in the summer and winter hemisphere is less than the sum of the north and south hemispheres at equinox. The greater globally-averaged Joule heating at equinox, and the thermal expansion, accounts for approximately one-half the modelled semi-annual variation.

The remaining semi-annual density variation suggests an alternative mechanism. It is suggested that the global scale, interhemispheric circulation at solstice mixes the major thermospheric species, analagous to a huge turbulent eddy. The effect causes less diffusive separation of species at solstice which tends to raise molecular nitrogen and oxygen densities and reduce atomic oxygen density, compared with equinox. The increased mean mass, at solstice, reduces the density scale height and leads to less atmospheric density at a given altitude. It is suggested that this compression of the atmosphere at solstice can explain a large fraction of the semi-annual density anomaly.

Further analysis reveals that the vertical profile of the amplitude of the semi-annual variation from the mixing mechanism in the physically- based model agrees well with MSIS. The implication is that little of the mean level of the semi-annual density variation is caused by temperature changes. Much of the variability from year to year in the amplitude could arise either from different globally-averaged heating rates in equinox and solstice, or from changing amplitudes of heating or turbulent mixing from the lower atmosphere sources. Further analysis on the solar cycle trend in the semi-annual variation will also be pursued.

OTHER ACTIVITIES

A paper entitled "Thermosphere and Ionosphere Dynamics during High Solar Activity Equinox Conditions" by F.A. Marcos, T. Fuller- Rowell, J.M. Forbes, and M. Codrescu was presented at the COSPAR Assembly on July 15, 1996, by T. Fuller-Rowell. This work primarily involved a comparison between SETA data and CTIM predictions during the March, 1979 storm period, and related interpretations. A number of figures depicting the latitude vs. time response of the thermospheric density, as revealed by the SETA data and as modelled by CTIM, were constructed for this presentation.